Preprints of the 21st IFAC World Congress (Virtual)
Berlin, Germany, July 12-17, 2020

A Comparative Study of Kalman-like Filters for State Estimation of Turning Aircraft in Presence of Glint Noise ⋆

Gennady Yu. Kulikov * **Maria V. Kulikova** *

* *CEMAT, Instituto Superior Técnico, Universidade de Lisboa, Av. Rovisco Pais 1, 1049-001 LISBOA, Portugal (emails: gennady.kulikov@tecnico.ulisboa.pt, maria.kulikova@ist.utl.pt).*

Abstract: This paper continues the study started by Kulikov and Kulikova on state estimation accuracies of various Kalman-like filtering techniques in target tracking scenarios with non-Gaussian noise in 2018. The cited authors examined a number of methods, which are grounded in the minimum-variance or maximum-correntropy criteria and cover extended-, cubature- and unscented-type Kalman filters, in the well-known turning aircraft scenario with impulsive (shot) noise or mixed-Gaussian one. Despite the success of the maximum-correntropy-based filtering methods reported on estimation of linear discrete-time stochastic systems in literature, those case studies expose the superiority of the cubature and unscented Kalman filters towards various extended Kalman methods designed in the minimum-variance sense or grounded in the maximum-correntropy criterion within the mentioned target tracking scenarios. Here, we extend that examination to the turning aircraft scenario with glint noise, which is simulated by a sum of two zero-mean Gaussian variables with difference covariances. In particular, our study reveals a valued potential of the maximum-correntropy-based accurate continuous-discrete extended Kalman filters devised by the above authors in this glint noise state estimation environment.

Keywords: Continuous-discrete nonlinear stochastic model, correntropy, Kalman-like filtering, radar tracking, maneuvering target, glint noise.

1. INTRODUCTION

Following Bar-Shalom et al. (2001); Li and Jilkov (2003) and many others, it is natural to simulate target tracking of airborne objects by means of a coupled continuous-discrete stochastic state-space system of the form

$$dX(t) = F\big(X(t)\big)dt + G(t)dW(t), \quad t > 0, \tag{1}$$

$$Z_k = h(X_k) + V_k, \quad k \geq 1. \tag{2}$$

Here, the process model is of continuous-time fashion and presented mathematically by an Itô-type *Stochastic Differential Equation* (SDE) of the form (1), in which the vector $X(t) \in \mathbb{R}^n$ of size n represents the state of the plant, the function $F : \mathbb{R}^n \to \mathbb{R}^n$ (termed the drift coefficient in this model) describes its state evolution in time, $G(t)$ is a diffusion matrix of size $n \times n$, which can be time-variant/-invariant depending on the target tracking scenario in use, and the disturbance $\{W(t),\, t > 0\}$ is the multivariate Brownian motion whose increment $dW(t)$ is the zero-mean white process with covariance $Q(t)dt > 0$ of size $n \times n$ being time-variant/-invariant, as well. Here, the initial state $X(0)$ is assumed to be a random variable with mean $\bar{X}_0$ and covariance Π_0. The discrete-time-fashion measurement model (2) simulates usually a digitalized flight control system, which can be based on a radar, sonar and so on. This equation links a new measurement information received in the form of vector $Z_k \in \mathbb{R}^m$ to the aircraft's state X_k, which implies the vector $X(t_k)$, by means of a sufficiently smooth function $h : \mathbb{R}^n \to \mathbb{R}^m$ at every *sampling time* t_k. Such airborne object's observations are considered to be noisy, that is simulated mathematically by the disturbance V_k given in the form of zero-mean white-noise random vectors with their covariance matrices $R_k > 0$. We emphasize that the sampling information arrives uniformly in a *sampling interval* of size δ in our study, below. All realizations of the noises $dW(t)$, V_k and the initial state $X(0)$ are assumed to be taken from mutually independent random distributions.

The classical theory developed for a suboptimal estimation of continuous-discrete stochastic systems (1) and (2) relies mostly on the Gaussianity assumption of the a priori and a posteriori random distributions of the plant's state X_k and its measurement Z_k. It allows various extended-, cubature- and unscented-type Kalman filters to be designed under the *minimum-variance* performance index, as shown in Jazwinski (1970); Arasaratnam et al. (2010); Särkkä and Sarmavuori (2013); Särkkä (2007); Kulikov and Kulikova (2016, 2017b,a, 2020a,b). Certainly, this Gaussianity assumption is not always realistic in applied science and engineering and state estimators intended for treating non-Gaussian random distributions are also of great interest. A novel approach to state estimation in non-Gaussian stochastic systems is grounded in the notion of *correntropy*

⋆ The authors acknowledge the financial support of the Portuguese FCT — *Fundação para a Ciência e a Tecnologia*, through the projects UIDB/04621/2020 and UIDP/04621/2020 of CEMAT/IST-ID, Center for Computational and Stochastic Mathematics, Instituto Superior Técnico, University of Lisbon.

introduced recently by Santamaria et al. (2006); Liu et al. (2007); Principe (2010). Its maximization underlies the development of a range of filtering methods in He et al. (2011); Chen et al. (2014, 2015); Wu et al. (2015); Izanloo et al. (2016); Chen et al. (2017); Liu et al. (2017); Kulikova (2017), which are robust to outliers and utilized with a success. Besides, the high performance of such maximum-correntropy-based filtering methods reported in the cited literature is observed mainly in linear discrete-time state estimation tasks. In addition, the further investigation of Kulikov and Kulikova (2018) reveals rather poor accuracies achieved with the *Extended Kalman Filtering* (EKF) grounded in the *Maximum-Correntropy Criterion* (MCC) in comparison to those of the *Cubature Kalman Filtering* (CKF) and *Unscented Kalman Filtering* (UKF) methods within the turning aircraft scenario with impulsive (shot) noise and mixed-Gaussian one, as well. That casts doubt on a potential MCC-based filtering's success in nonlinear state estimation scenarios of the form (1) and (2).

In this paper, we fulfil a comparative case study of all the filters discussed by Kulikov and Kulikova (2018), within the air traffic control scenario of Arasaratnam et al. (2010), but implemented with a glint measurement noise, here. The glint phenomenon is well-known and observed often in practical radar performances. It is caused by irregular electromagnetic wave reflections addressed in Hewer et al. (1987). Nowadays, we are familiar with different mathematical representations of target glint noise, as those elaborated in Borden and Mumford (1983); Wu and Cheng (1994); Li and Jilkov (2005); Bilik and Tabrikian (2006). Below, we stick to its particular simulation in the form of a sum of two zero-mean Gaussian variables, in which one is realized with high probability but small variance and the other with low probability but high variance (see further details in Hewer et al. (1987); Wu (1993); Bilik and Tabrikian (2006); Kulikov and Kulikova (2020a)). The main issue of our interest is an assessment of state estimation potential of the mentioned Kalman-like filters within this challenging turning aircraft scenario corrupted by a glint noise disturbance.

2. TURNING AIRCRAFT SCENARIO WITH GLINT MEASUREMENT NOISE

In line with Arasaratnam et al. (2010), we consider below a target tracking scenario in which an aircraft turning in the horizontal plane is being observed by a radar located at the origin. First, the target's dynamic behavior is assumed to obey the SDE model (1) whose state vector is $X(t) := [\, x(t)\ \dot{x}(t)\ y(t)\ \dot{y}(t)\ z(t)\ \dot{z}(t)\ \omega(t)\,]^\top \in \mathbb{R}^7$ with the entries $x(t)$, $y(t)$, $z(t)$ referring to the airborne object's position, the entries $\dot{x}(t)$, $\dot{y}(t)$, $\dot{z}(t)$ meaning its velocity (both in the Cartesian coordinates) at time t and ω standing for the (almost) constant turn rate of the aircraft. Second, the coordinated turn of the target is simulated by the drift function $F\big(X(t)\big) := [\, \dot{x}(t)\ -\omega(t)\dot{y}(t)\ \dot{y}(t)\ \omega(t)\dot{x}(t)\ \dot{z}(t)\ 0\ 0\,]^\top \in \mathbb{R}^7$ in this case study. Furthermore, it is corrupted by the additive noise $W(t) \in \mathbb{R}^7$, which is is a multivariate Wiener process with independent zero-mean Gaussian increments $dW(t)$, whose covariance is the diagonal matrix $I_7 dt$ with I_7 denoting the identity matrix of size 7. Again, in line with the scenario of Arasaratnam et al. (2010), the diffusion matrix G is set to be time-invariant, diagonal and of the form $G := \mathrm{diag}\{\, 0\ \sigma_1\ 0\ \sigma_1\ 0\ \sigma_1\ \sigma_2\,\}$ with $\sigma_1 := \sqrt{0.2}\,\mathrm{m/s}$ and $\sigma_2 := 0.007^\circ/\mathrm{s}$ in the present glint-noise case study.

Next, Arasaratnam et al. (2010) employ the measurement equation (2) in which, first, the data observed takes the form of vector $Z_k := [\, r_k\ \theta_k\ \phi_k\,]^\top \in \mathbb{R}^3$ and, second, the measurement function obeys the following formula:

$$h\big(X_k\big) := \begin{bmatrix} \sqrt{x_k^2 + y_k^2 + z_k^2} \\ \tan^{-1}(y_k/x_k) \\ \tan^{-1}\Big(z_k/\sqrt{x_k^2 + y_k^2}\Big) \end{bmatrix} \in \mathbb{R}^3$$

where the aircraft's coordinates x_k, y_k, z_k present its space position at the sampling time t_k. This measurement model implies that the radar in use is equipped for measuring the range r, the azimuth angle θ and the elevation angle ϕ.

As already said above, our target tracking scenario assumes noisy measurements Z_k corrupted with a glint noise. Then, following Hewer et al. (1987); Wu (1993); Bilik and Tabrikian (2006); Kulikov and Kulikova (2020a), this measurement disturbance is simulated as follows:

$$V_k := (1 - p_g)\,\mathcal{N}(0, R_m) + p_g\,\mathcal{N}(0, R_g). \tag{3}$$

In Eq. (3), the zero-mean Gaussian variable $\mathcal{N}(0, R_m)$ represents the uncertainty of radar measurements, the other one $\mathcal{N}(0, R_g)$ models the glint phenomenon and the scalar p_g denotes the probability of the glint. In line with the cited literature, the covariance R_m of the radar measurement noise is considered to be standard, i.e. as in Arasaratnam et al. (2010), it is taken to be diagonal and of the form $R_m := \mathrm{diag}\big\{\, \sigma_r^2\ \sigma_\theta^2\ \sigma_\phi^2\,\big\}$ where $\sigma_r = 50$ m, $\sigma_\theta = 0.1^\circ$, $\sigma_\phi = 0.1^\circ$. However, the covariance of the target glint outliers must be large. That is why we merely increase the radar measurement covariance with a factor of 100, i.e. set $R_g := 100 R_m$ in our case study, below. We stress that the covariance R_k in the measurement model (2) with the glint-noise disturbance (3) is considered to be time-invariant and evaluated statistically from the sampled noise sequence V_k in each Monte Carlo simulation.

The scenario in use follows Arasaratnam et al. (2010) and considers that the initial state of the target obeys the Gaussian distribution $X_0 \sim \mathcal{N}(\bar{X}_0, \Pi_0)$ with the mean $\bar{X}_0 := [\, 1000\,\mathrm{m}\ \ 0\,\mathrm{m/s}\ \ 2650\,\mathrm{m}\ \ 150\,\mathrm{m/s}\ \ 200\,\mathrm{m}\ \ 0\,\mathrm{m/s}\ \ 6^\circ/\mathrm{s}\,]^\top$, and covariance $\Pi_0 := I_7/100$. It is treated by Kalman filters outlined briefly in Sec. 3 in the time interval $[0, 160\ \mathrm{s}]$.

3. BRIEF DESCRIPTION OF KALMAN-LIKE FILTERING METHODS UNDER EXAMINATION

All state estimation algorithms examined in the above-described glint-noise-air-traffic-control scenario are applicable to continuous-time stochastic systems of the form (1) with discrete-time measurements of the form (2). These are devised under the minimum-variance optimization criterion or under the maximum-correntropy performance index as well. More precisely, our case study covers various versions of the EKF, CKF and UKF techniques, which are presented both in the conventional (non-square-root) form and in the square-root one and elaborated with all necessary particulars in Kulikov and Kulikova (2018) and references therein. In Sec. 3, we outline briefly all the state

estimation algorithms under consideration and refer the interested reader for further details to the cited literature.

3.1 Minimum-Variance-Based Extended Kalman Filters

The minimum-variance-based extended Kalman filtering was designed long ago and presented briefly in the form of Theorem 8.1 in Jazwinski (1970). The cited result is grounded in application of the known continuous-time filter of Kalman and Bucy (1961) to the nonlinear stochastic system (1) and (2) linearized around the filtering solution at each sampling time t_k. This allows the EKF to be split into two stages: the time and measurement updates.

The time update (or prediction) step of the EKF under consideration is based on the time evolution of the mean and covariance of the random distribution propagated in line with the *Moment Differential Equations* (MDE):

$$\frac{d\hat{X}(t)}{dt} = F\big(\hat{X}(t)\big), \tag{4}$$

$$\frac{dP(t)}{dt} = J\big(\hat{X}(t)\big)P(t) + P(t)J^{\top}\big(\hat{X}(t)\big) + GQG^{\top}, \tag{5}$$

in which the matrix $J(\hat{X}(t))$ refers to the derivative (Jacobian) of the drift coefficient in SDE (1). This Jacobian matrix is evaluated at the expected trajectory in every sampling interval $[t_{k-1}, t_k]$. The diffusion and covariance matrices G and Q have been already presented in Sec. 2.

Having used the filtering solution $\hat{X}_{k-1|k-1}$ and $P_{k-1|k-1}$ as the initial values in MDE (4), (5), one solves the set problem by means of any appropriate numerical integration method and, then, the numerical solution derived at the end point of the integration interval $[t_{k-1}, t_k]$ is taken as the predicted state expectation $\hat{X}_{k|k-1}$ and covariance $P_{k|k-1}$ at each sampling time t_k. The measurement update (or correction) step of the EKF methods under consideration can be fulfilled in the conventional (i.e. non-square-root) form or in the square-root one as explained in Sec. 4.1 and 4.2 of Kulikov and Kulikova (2018), respectively.

This theory allows the following two EKF-based filters (and their acronyms) to be included in our case study:

- `ACD-EKF` is the acronym of the ACD-EKF method grounded in the NIRK formula of order 6 (see Sec. 2.2 in Kulikov and Kulikova (2017a) for more details);
- `ACD-EKF(sr)` is the acronym of the square-root version of `ACD-EKF` described above (see Sec. 3 in Kulikov and Kulikova (2017b) for further details).

3.2 Maximum-Correntropy-Based Extended Kalman Filters

The *correntropy* is a novel random variable similarity measure introduced by Santamaria et al. (2006); Liu et al. (2007); Principe (2010), which leads to the MCC-based EKF built for treating stochastic systems (1) and (2) in Sec. 3 of Kulikov and Kulikova (2018). The time update steps of such filters are grounded in the numerical integration of the same MDE (4) and (5), whereas their measurement update steps differ. These are presented in full detail and explained in the cited paper. In particular, the practical performance of the MCC-based EKF methods depends on the size $\sigma > 0$ of the kernel (bandwidth), which is utilized in the MCC implemented here and can be adaptive or fixed. That is why we include the following six filters (and their acronyms) in our glint-noise case study:

- `MCC(ad)-ACD-EKF` is the acronym of the MCC-based ACD-EKF with the adaptive kernel size σ (see more details in Sec. 3.1 of Kulikov and Kulikova (2018));
- `MCC(80)-ACD-EKF` is the acronym of the MCC-based ACD-EKF with the prefixed kernel size σ (see more details in Sec. 3.1 of Kulikov and Kulikova (2018));
- `IMCC(ad)-ACD-EKF` is the acronym of the IMCC-based ACD-EKF with the adaptive kernel size σ (see details in Sec. 3.1 of Kulikov and Kulikova (2018));
- `IMCC(80)-ACD-EKF` is the acronym of the IMCC-based ACD-EKF with the prefixed kernel size σ (see details in Sec. 3.1 of Kulikov and Kulikova (2018));
- `IMCC(ad)-ACD-EKF(sr)` is the acronym of the square-root IMCC-based ACD-EKF with the adaptive kernel size σ (see Sec. 3.2 in Kulikov and Kulikova (2018));
- `IMCC(80)-ACD-EKF(sr)` is the acronym of the square-root IMCC-based ACD-EKF with the prefixed kernel size σ (see Sec. 3.2 in Kulikov and Kulikova (2018)).

3.3 Minimum-Variance-Based Cubature Kalman Filters

The CKF methods in use are grounded in the third-degree spherical-radial cubature rule and implemented always in the square-root form. These can be built within the *continuous-discrete* and *discrete-discrete* approaches. In the first one, the evolution of the mean and covariance obeys the MDE, again, but such equations have a more complicated and coupled form, which requires advanced numerical integration solvers with automatic local and global error controls to be applied as explained in Kulikov and Kulikova (2017b). The cited paper also presents the mixed-type filter based on the EKF and CKF techniques. The second approach relies on application of SDE discretization schemes, as those in Arasaratnam et al. (2010). It entails equidistant sampling interval subdivisions to be implemented. In other words, all such state estimators are of the m-step fashion, where m is the number of equal numerical integration steps fulfilled in each sampling period $[t_{k-1}, t_k]$. In our glint-noise case study, we include and examine the following CKF methods and their acronyms:

- `ACD-ECKF(sr)` is the square-root ACD-ECKF method designed in Sec. 4 of Kulikov and Kulikova (2017b);
- `ACD-CKF(sr)` is the square-root ACD-CKF method presented in Sec. 2 of Kulikov and Kulikova (2017b);
- `CD-CKF256(sr)` and `CD-CKF512(sr)` are the square-root CD-CKF methods implemented with 256 and 512 equidistant subdivisions of sampling interval (see details in Sec. II-A of Kulikov and Kulikova (2016)).

3.4 Minimum-Variance-Based Unscented Kalman Filters

The UKF-like methods under consideration are close to the state estimators outlined briefly in Sec. 3.3, but these are grounded in the unscented transform instead and implemented always in the conventional (i.e. non-square-root) form. All such filtering techniques are also constructed within the same *continuous-discrete* and *discrete-discrete* approaches, which admit the variable- and fixed-stepsize implementations and the mixed-type version based on the

EKF and UKF methods, as well. In our glint-noise-air-traffic-control case study, we include and examine the following UKF-type methods and their acronyms:

- `ACD-EUKF` is the mixed-type ACD-EUKF algorithm designed in Sec. 2.3 of Kulikov and Kulikova (2017a);
- `ACD-UKF` is the acronyms of the ACD-UKF algorithm presented in Sec. 2.1 of Kulikov and Kulikova (2017a);
- `CD-UKF256` and `CD-UKF512` are the CD-UKF methods implemented with 256 and 512 equidistant subdivisions of every sampling interval, respectively (see details in Sec. II-B of Kulikov and Kulikova (2016)).

4. SIMULATION RESULTS

We assess performances of the filters outlined briefly in Sec. 3 in severe conditions of tackling the 7-dimensional radar tracking scenario of Arasaratnam et al. (2010), where an aircraft executes the coordinated turn, but implemented here with the glint noise discussed in Sec. 2 in detail. We further skip other particulars of our target tracking case study, and refer the interested reader to those elaborated in Kulikov and Kulikova (2018), which are similar to the present glint-noise scenario. All the methods under consideration are coded and run in MATLAB.

Following Kulikov and Kulikova (2018), the accuracies of all the state estimation methods are assessed in the sense of the *Accumulated Root Mean Square Errors* in position (ARMSE_p) and in velocity (ARMSE_v) defined as follows:

$$\mathrm{ARMSE}_p := \Big[\frac{1}{100K}\sum_{mc=1}^{100}\sum_{k=1}^{K}\big(x_{mc}^{\mathrm{true}}(t_k)-\hat{x}_{k|k}^{mc}\big)^2 + \big(y_{mc}^{\mathrm{true}}(t_k)-\hat{y}_{k|k}^{mc}\big)^2+\big(z_{mc}^{\mathrm{true}}(t_k)-\hat{z}_{k|k}^{mc}\big)^2\Big]^{1/2},$$

$$\mathrm{ARMSE}_v := \Big[\frac{1}{100K}\sum_{mc=1}^{100}\sum_{k=1}^{K}\big(\dot{x}_{mc}^{\mathrm{true}}(t_k)-\hat{\dot{x}}_{k|k}^{mc}\big)^2 + \big(\dot{y}_{mc}^{\mathrm{true}}(t_k)-\hat{\dot{y}}_{k|k}^{mc}\big)^2+\big(\dot{z}_{mc}^{\mathrm{true}}(t_k)-\hat{\dot{z}}_{k|k}^{mc}\big)^2\Big]^{1/2}$$

where $x_{mc}^{\mathrm{true}}(t_k)$, $y_{mc}^{\mathrm{true}}(t_k)$, $z_{mc}^{\mathrm{true}}(t_k)$ and $\dot{x}_{mc}^{\mathrm{true}}(t_k)$, $\dot{y}_{mc}^{\mathrm{true}}(t_k)$, $\dot{z}_{mc}^{\mathrm{true}}(t_k)$ stand for the aircraft's position and velocity simulated by the Euler-Maruyama method with the small step size $\tau := 0.0005$ at time t_k in the mc-th Monte Carlo run (out of 100 independent simulations), $\hat{x}_{k|k}^{mc}$, $\hat{y}_{k|k}^{mc}$, $\hat{z}_{k|k}^{mc}$ and $\hat{\dot{x}}_{k|k}^{mc}$, $\hat{\dot{y}}_{k|k}^{mc}$, $\hat{\dot{z}}_{k|k}^{mc}$ denote the aircraft's position and velocity estimated by each filter, k means the particular sampling time t_k and K refers to the total number of samples in the simulation interval $[0, 160\,\mathrm{s}]$. The sampling periods utilized are $\delta = 2, 4, \ldots, 20\,\mathrm{s}$, and, following Bilik and Tabrikian (2006), the glint-noise probability is set to be $p_g = 0.25$ in our glint-noise-air-traffic-control scenario.

The filters' accuracies observed in this glint-noise radar tracking case study are shown in the logarithmically-scaled Fig. 1(a-d). First, these plots expose the superiority of the variable- and fixed-stepsize CKF- and UKF-type filtering algorithms when the discretization error is small enough (i.e. the number m of sampling interval subdivisions is sufficiently large). We emphasize that this condition holds automatically in `ACD-UKF` and `ACD-CKF(sr)` and these produce decent state estimates for all the sampling rates δ utilized in the case study in Sec. 4. Besides, if the subdivision number m predefined by the user is insufficient the fixed-stepsize methods produce poor state estimates with large ARMSE_p and ARMSE_v for long sampling periods, as those committed by `CD-UKF256` and `CD-CKF256(sr)` at $\delta \geq 14$ s. The same reason counts in favor of the variable-stepsize CKF and UKF methods in this target tracking scenario with low sampling rates in comparison to their fixed-stepsize counterparts `CD-UKF512` and `CD-CKF512(sr)` (see Fig. 1(c,d)). In general, the higher accuracy of the variable- and fixed-stepsize CKF and UKF methods reported in our experiment is explained by more accurate approximations of the time- and measurement-updated mean and covariance achieved within these techniques and their applicability to treating non-Gaussian stochastic systems of the form (1) and (2), as well. Second, all the EKF-type methods are less accurate and underperform the above-discussed CKF and UKF. Nevertheless, the best accuracy is observed for the MCC-based EKF methods with the adaptive kernel size among this family of filtering algorithms in our radar tracking scenario with glint noise (3). Eventually, these filters can be a good choice because of their low computational complexity exhibited in Fig. 1(e,f). Third, the remaining EKF techniques lose considerably the above-elaborated filters (especially, in the sense of ARMSE_v reported in Fig. 1(c,d)) and hardly suit for decent estimation of stochastic systems with glint noise.

Next, we pay more attention to the efficiency of all the filtering algorithms under examination. Here, we assess and compare the *average filtering time* out of 100 Monte Carlo simulations. This time is displayed in Fig. 1(e,f). First, the latter plots show that the variable-stepsize methods `ACD-CKF(sr)` and `ACD-UKF`, which are the most accurate ones, are really time-consuming and slow. This is explained by the size of the MDE solved within these techniques. Kulikov and Kulikova (2017b,a, 2018) already mentioned that the filters under consideration integrate numerically the MDE, which are of size 98 and 105 in our glint-noise-air-traffic-control scenario, respectively. Second, all the EKF-based and mixed-type filters treat the MDE of size 7, only. That is why the latter methods are much less time-consuming and even expose the similar computational effort. On the other hand, they are less accurate in comparison to `ACD-CKF(sr)` and `ACD-UKF`. Third, the fixed-stepsize `CD-CKF256(sr)`, `CD-CKF512(sr)`, `CD-UKF256` and `CD-UKF512` are also rather accurate in the present glint-noise scenario. However, such filtering algorithms are not self-adaptive and can fail when the process model and/or sampling rate change, as evidenced by Kulikov and Kulikova (2016, 2017b,a, 2018). Fourth, as a potential compromise between the accuracy and efficiency, the MCC-based EKF methods with the adaptive kernel size σ may succeed and be recommended for practical use in state estimation tasks of applied science and engineering.

5. CONCLUSION

This paper has continued the study started by Kulikov and Kulikova (2018) on the state estimation performance of various Kalman-like filtering techniques in nonlinear target tracking scenarios with non-Gaussian noise. Following the cited authors, we have examined a number of methods, which are grounded in the minimum-variance or maximum-correntropy criteria and cover extended-,

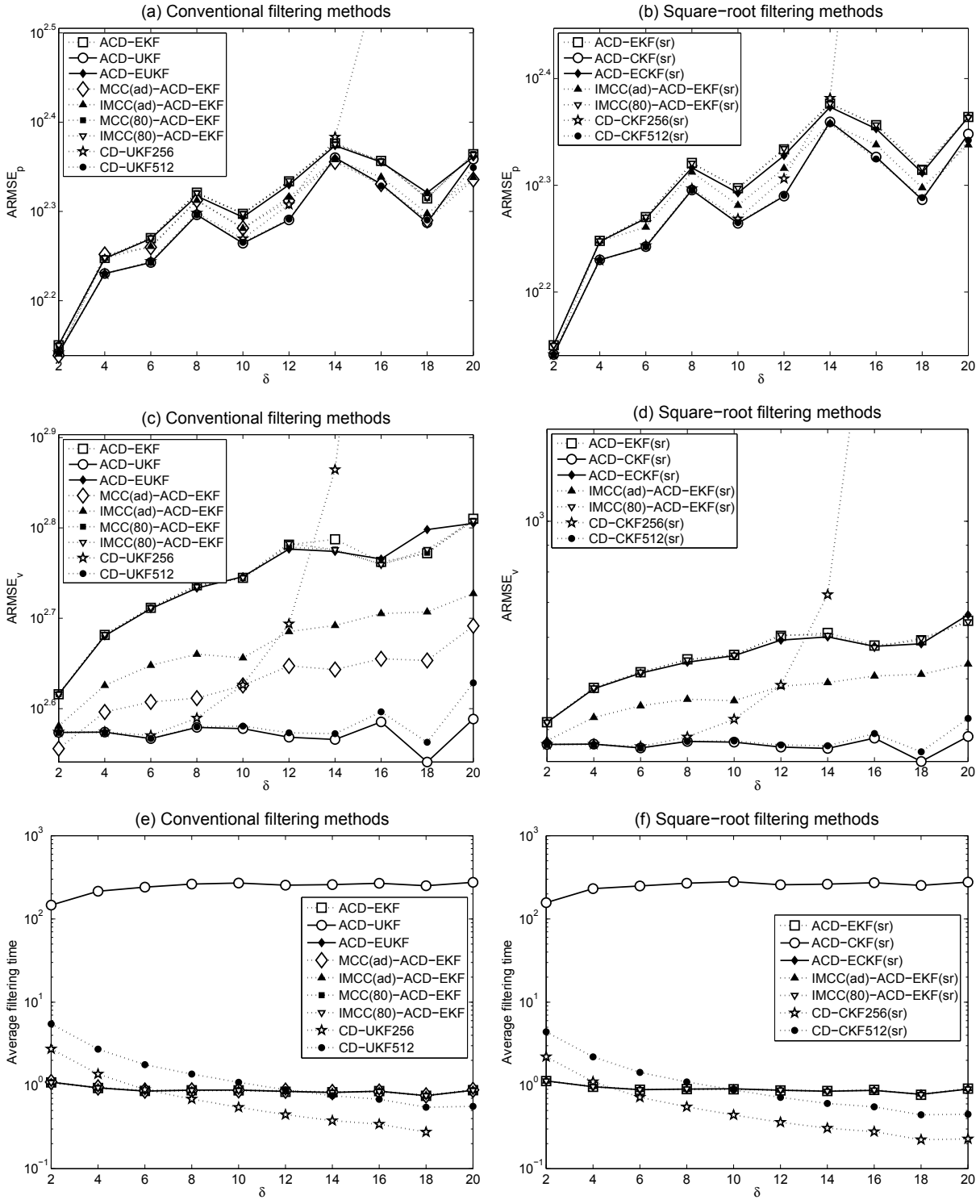

Fig. 1. The accuracy and efficiency comparison of the minimum-variance- and maximum-correntropy-based Kalman-like filtering methods in the air traffic control scenario with glint noise (3).

cubature- and unscented-type Kalman filtering techniques. These have been applied for treating the famous turning aircraft scenario but implemented presently with glint noise. This glint noise has been modeled by a sum of two zero-mean Gaussian variables with difference covariances in our case study. The numerical examination fulfilled has revealed the superiority of the cubature and unscented Kalman filtering methods towards various extended Kalman filters designed in the minimum-variance sense or grounded in the maximum-correntropy criterion within our target tracking scenario. At the same time, the maximum-correntropy-based accurate continuous-discrete extended Kalman filters with the adaptive kernel size also expose a decent state estimation potential in treating target tracking scenarios with the glint noise. Most importantly, their low computational burden makes such methods preferable in state estimation tasks of large size.

REFERENCES

Arasaratnam, I., Haykin, S., and Hurd, T.R. (2010). Cubature Kalman filtering for continuous-discrete systems: Theory and simulations. *IEEE Trans. Signal Process.*, 58(10), 4977–4993.

Bar-Shalom, Y., Li, X.R., and Kirubarajan, T. (2001). *Estimation with Applications to Tracking and Navigation.* Wiley, New York.

Bilik, I. and Tabrikian, J. (2006). Target tracking in Glint noise environment using nonlinear non-Gaussian Kalman filter. In *Proceedings of the 2006 IEEE Conference on Radar*, 282–286.

Borden, B. and Mumford, M. (1983). A statistical glint/radar cross section target model. *IEEE Trans. Aerosp. Electron. Syst.*, 19(5), 781–785.

Chen, B., Liu, X., Zhao, H., and Príncipe, J.C. (2017). Maximum correntropy Kalman filter. *Automatica*, 76, 70–77.

Chen, B., Wang, J., Zhao, H., Zheng, N., and Príncipe, J.C. (2015). Convergence of a fixed-point algorithm under maximum correntropy criterion. *IEEE Signal Process. Lett.*, 22(10), 1723–1727.

Chen, B., Xing, L., Liang, J., Zheng, N., and Príncipe, J.C. (2014). Steady-state mean-square error analysis for adaptive filtering under the maximum correntropy criterion. *IEEE Signal Process. Lett.*, 21(7), 880–884.

He, R., Zheng, W.S., and Hu, B.G. (2011). Maximum correntropy criterion for robust face recognition. *IEEE Trans. Pattern Anal. Mach. Intell.*, 33(8), 1561–1576.

Hewer, G.A., Martin, R.D., and Zeh, J. (1987). Robust preprocessing for Kalman filtering of glint noise. *IEEE Trans. Aerosp. Electron. Syst.*, AES-23(1), 120–128.

Izanloo, R., Fakoorian, S.A., Yazdi, H.S., and Simon, D. (2016). Kalman filtering based on the maximum correntropy criterion in the presence of non-Gaussian noise. In *Proceedings of 2016 Annual Conference on Information Science and Systems (CISS)*, 500–505.

Jazwinski, A.H. (1970). *Stochastic Processes and Filtering Theory.* Academic Press, New York.

Kalman, R.E. and Bucy, R.S. (1961). New results in linear filtering and prediction theory. *ASME J. Basic Eng.*, 83(1), 95–108.

Kulikov, G.Yu. and Kulikova, M.V. (2016). The accurate continuous-discrete extended Kalman filter for radar tracking. *IEEE Trans. Signal Process.*, 64(4), 948–958.

Kulikov, G.Yu. and Kulikova, M.V. (2017a). Accurate continuous-discrete unscented Kalman filtering for estimation of nonlinear continuous-time stochastic models in radar tracking. *Signal Process.*, 139, 25–35.

Kulikov, G.Yu. and Kulikova, M.V. (2017b). Accurate cubature and extended Kalman filtering methods for estimating continuous-time nonlinear stochastic systems with discrete measurements. *Appl. Numer. Math.*, 111, 260–275.

Kulikov, G.Yu. and Kulikova, M.V. (2018). Estimation of maneuvering target in the presence of non-Gaussian noise: A coordinated turn case study. *Signal Process.*, 145, 241–257.

Kulikov, G.Yu. and Kulikova, M.V. (2020a). Square-root accurate continuous-discrete extended-unscented Kalman filtering methods with embedded orthogonal and J-orthogonal QR decompositions for estimation of nonlinear continuous-time stochastic models in radar tracking. *Signal Process.*, 166, 107253.

Kulikov, G.Yu. and Kulikova, M.V. (2020b). NIRK-based Cholesky-factorized square-root accurate continuous-discrete unscented Kalman filters for state estimation in nonlinear continuous-time stochastic models with discrete measurements. *Appl. Numer. Math.*, 147, 196–221.

Kulikova, M.V. (2017). Square-root algorithms for maximum correntropy estimation of linear discrete-time systems in presence of non-Gaussian noise. *Systems and Control Letters*, 108, 8–15.

Li, X. and Jilkov, V. (2003). Survey on maneuvering target tracking. Part I: Dynamic models. *IEEE Trans. Aerosp. Electron. Syst.*, 39(4), 1333–1364.

Li, X. and Jilkov, V. (2005). Survey on maneuvering target tracking. Part V: Multiple-model methods. *IEEE Trans. Aerosp. Electron. Syst.*, 41(4), 1255–1321.

Liu, W., Pokharel, P.P., and Principe, J.C. (2007). Correntropy: Properties and applications in non-Gaussian signal processing. *IEEE Trans. Signal Process.*, 58(11), 5286–5298.

Liu, X., Qu, H., Zhao, J., and Chen, B. (2017). State space maximum correntropy filter. *Signal Process.*, 130, 152–158.

Principe, J. (2010). *Information Theoretic Learning: Renyi's Entropy and Kernel Perspectives.* Springer, New York.

Santamaria, I., Pokharel, P.P., and Principe, J.C. (2006). Generalized correlation function: Definition, properties, and application to blind equalization. *IEEE Trans. Signal Process.*, 54(6), 2187–2197.

Särkkä, S. (2007). On unscented Kalman filter for state estimation of continuous-time nonlinear systems. *IEEE Trans. Automat. Contr.*, 52(9), 1631–1641.

Särkkä, S. and Sarmavuori, J. (2013). Gaussian filtering and smoothing for continuous-discrete dynamic systems. *Signal Process.*, 93, 500–510.

Wu, W.R. (1993). Target tracking with glint noise. *IEEE Trans. Aerosp. Electron. Syst.*, 29(1), 174–185.

Wu, W.R. and Cheng, P.P. (1994). Nonlinear IMM algorithm for maneuvering target tracking. *IEEE Trans. Aerosp. Electron. Syst.*, 30(3), 875–886.

Wu, Z., Shi, J., Zhang, X., Ma, W., and Chen, B. (2015). Kernal recursive maximum correntropy. *Signal Process.*, 117, 11–16.